Microchimica Acta (2019) 186: 575
https://doi.org/10.1007/s00604-019-3570-y

ORIGINAL PAPER

A "turnon" aptasensor for simultaneous and time-resolved fluorometric determination of zearalenone, trichothecenes A and aflatoxin B_1 using WS_2 as a quencher

Sobia Niazi[1,2,3,4] · Imran Mahmood Khan[1,2,3,4] · Ye Yu[5] · Imran Pasha[6] · Muhammad Shoaib[1,2] · Ali Mohsin[7] · Bilal Sajid Mushtaq[1,2] · Wasim Akhtar[1,2] · Zhouping Wang[1,2,3,4]

Received: 27 December 2018 / Accepted: 2 June 2019 / Published online: 24 July 2019

Abstract

A "turn on" time-resolved fluorometric aptasensor is described for the simultaneous detection of zearalenone (ZEN), trichothecenes A (T-2), and aflatoxin B_1 (AFB_1). Multicolor-emissive nanoparticles doped with lanthanide ions (Dy^{3+}, Tb^{3+}, Eu^{3+}) were functionalized with respective aptamers and applied as a bioprobe, and tungsten disulfide (WS_2) nanosheets are used as a quencher of time-resolved fluorescence. The assay exploits the quenching efficiency of WS_2 and the interactions between WS_2 and the respective DNA aptamers. The simultaneous recognition of the three mycotoxins can be performed in a single solution. In the absence of targets, WS_2 is easily adsorbed by the mixed bioprobes via van der Waals forces between nucleobases and the WS_2 basal plane. This brings the bioprobe and WS_2 into close proximity and results in quenched fluorescence. In the presence of targets, the fluorescence of the bioprobes is restored because the analytes react with DNA probe and modify their molecular conformation to weaken the interaction between the DNAs and WS_2. Under the optimum conditions and at an excitation wavelength of 273 nm, the time-resolved fluorescence intensities (peaking at 488, 544 and 618 nm and corresponding to emissions of Dy^{3+}, Tb^{3+} and Eu^{3+}) were used to quantify ZEN, T-2 and AFB_1, respectively, with detection limits of 0.51, 0.33 and 0.40 pg mL^{-1} and a linear range from 0.001 to 100 ng mL^{-1}. The three mycotoxins can be detected simultaneously without mutual interference. The assay was applied to the quantification of ZEN, T-2 and AFB_1 in (spiked) maize samples. This homogeneous aptamer based assay can be performed within 1 h. Conceivably, it can become an alternative to other heterogeneous methods such as the respective enzyme-linked immunosorbent assays.

Keywords Lanthanide doped inorganic nanoparticles · Aptamer · Tungsten disulfide nanosheet · Homogeneous assay · Mycotoxins

Introduction

Mycotoxins are naturally occurring secondary metabolites that are produced by fungi during their growth [1]. The most common mycotoxins found in maize include ochratoxin A, aflatoxins (especially aflatoxin B_1), T-2 toxin, and zearalenone [2]. In this study, ZEN, T-2 and AFB_1 were chosen as targets to monitor in maize due to their severe damage and toxicity to

Electronic supplementary material The online version of this article (https://doi.org/10.1007/s00604-019-3570-y) contains supplementary material, which is available to authorized users.

✉ Zhouping Wang
wangzp@jiangnan.edu.cn

[1] State Key Laboratory of Food Science and Technology, Jiangnan University, Wuxi, China

[2] School of Food Science and Technology, Jiangnan University, Wuxi, China

[3] International Joint Laboratory on Food Safety, Jiangnan University, Wuxi, China

[4] Synergetic Innovation Center of Food Safety and Quality Control of Jiangsu Province, Jiangsu, China

[5] Technology Center of Zhangjiagang Entry-Exit Inspection and Quarantine Bureau, Zhangjiagang, China

[6] National Institute of Food Science and Technology, University of Agriculture, Faisalabad, Pakistan

[7] State Key Laboratory of Bioreactor Engineering, East China University of Science and Technology, Shanghai, China

human health. ZEN can affect the mammal's reproductive system in terms of decreased fertility and abortions [3]. T-2 toxins are toxic to the immune system and also cause cytotoxic and immunosuppressive injury by preventing RNA and DNA synthesis [4]. AFB_1 are the most toxic and predominant mycotoxins which are classified as a Group 1 carcinogen by the International Agency for Research on Cancer (IARC) due to their carcinogenic, teratogenic and mutagenic potential [5]. Consequently, the development of a sensitive, easy-to-use and rapid assay for the quantification of multiple mycotoxins in cereals is highly desirable in agro-food analysis.

Conventional methods including high-performance liquid chromatography, gas chromatography-mass spectrometry and liquid chromatography tandem mass spectrometry [6, 7] have been established for screening of mycotoxins. Although these techniques offer sufficient accuracy, sensitivity and good repeatability, laborious sampling and trained personnel are required for measurements. Antibodies-based immunoassays i.e. microarray-based immunoassay [2], enzyme-linked immunosorbent assay [8], time-resolved fluoroimmunoassay [9], time-resolved fluorescent immunochromatography analysis [10] have been used as simple, fast and effective methods for detection of mycotoxin. However, antibodies are obtained from an expensive and long procedure and also antibodies are vulnerable to the environment, leading to poor detection performances. Thus, it is a great challenge to accomplish sensitive and rapid simultaneous recognition of mycotoxins in real samples.

Lanthanide doped inorganic nanoparticles have been recommended as an encouraging innovative type of fluorescent probes. The Ln^{3+}-doped time-resolved fluorescence nanoparticles (TRFNPs) possess following advantages, such as favorable biocompatibility, resistance to photobleaching, high chemical stability, low cytotoxicity, multicolor doping, controlled and simple synthesis, large Stokes shifts, and extensive fluorescence lifetimes [11]. These characteristics can elude the overlap between the emission and excitation spectra of the fluorophore; therefore, can be used to develop a new fluorescence bioprobes for food safety assays. Moreover, using the long life time fluorescence emission of Ln^{3+} ion compounds can diminish the background noises efficiently. Thus, as compared to conventional fluorescent assays, time-resolved fluorescent assay offers high signal-to-noise ratio in fluorescence based biodetection. Furthermore, aptamers comparable to antibodies can also offer features such as high binding affinity to targets, easier synthesis, lower immunogenicity, smaller size, versatile chemistry and better thermal stability [12]. As compare to biosensors using natural receptors i.e. enzymes and antibodies, the aptamer based biosensor have following benefits i.e. high specificity, chemical stability, high affinity to targets, high purity and reproducibility through commercial synthesis and great flexibility [13]. In combination with aptamers, lanthanides and their complexes were used as signaling units. They have been used in the aptasensors to detect *Staphylococcus aureus* enterotoxins [14], ricin [15] and *Salmonella typhimurium* [16]. Conversely, its grouping with aptamers for detection of mycotoxin has not been studied so far.

WS_2 nanomaterial, which is 2D layered and has S-W-S sandwich structures, is one of the newly emergent transition metal dichalcogenides (TMDC) [17]. Up to now, only few WS_2 nanosheet-based bioassays have been reported [18, 19], mostly related with quenching of dye by WS_2 [18, 20, 21]. As reported by the previous works, WS_2 has been applied in fluorescence based assays due to its differential affinity towards single stranded and double-stranded DNA (ssDNA and dsDNA) [21, 22], but the applications in time-resolved fluorescence aptasensor is not very common. Thus, there is an urgent necessity to discover the new use of WS_2 as fluorescence quencher for time-resolved fluorescence in the area of biosensor. Moreover, WS_2 presented extraordinarily high fluorescence quenching efficiency over grapheme oxide, which is very important for the sensitivity of quenching and recovery based biosensor [21]. Consequently, inspired by the above findings, we believe that WS_2 can be applied as fluorescence quencher for quenching and restoration based biosensor for the detection of ZEN, T-2 and AFB_1.

In this study, a new "turn on" aptasensor was designed (Fig. 1) for sensitive and rapid simultaneous recognition of three mycotoxins (ZEN, T-2 and AFB_1). Herein, simultaneous detection were carried out using aptamers as specific detection element conjugated to Ln^{3+} ($Ln^{3+} = Dy^{3+}$, Tb^{3+}, Eu^{3+}) doped TRFNPs and WS_2 as fluorescence quencher. The presented aptasensor indicate the novel use of strong fluorescence and long lifetime of TRFNPs and also unique quenching efficiency of WS_2 for the quantitative analysis of mycotoxins. Besides, the method can quantify ZEN, T-2 and AFB_1 in real sample. The aptasensor has been confirmed to display high sensitivity, high-throughput and appropriate simultaneous recognition of three mycotoxins.

Materials and methods

Reagents

$YCl_3.6H_2O$ was obtained from Aladdin chemistry Co. Ltd. (Shanghai, China) (http://www.aladdin-e.com). $EuCl_3.6H_2O$, $TbCl_3.6H_2O$ and $DyCl_3.6H_2O$ were bought from Sigma-aldrich (www.sigmaaldrich.com). Polyethylenimine (PEI, ca. 30% in water) was obtained from TCI (Shanghai, China) Development Co., Ltd. (http://www.tcic hemicals.com). The glutaraldehyde solution (25% in *V*/V), ethylene glycol, KCl, NH_4F, ethanol and all the chemicals used for solutions and buffers preparation were purchased from Sinopahrm chemical

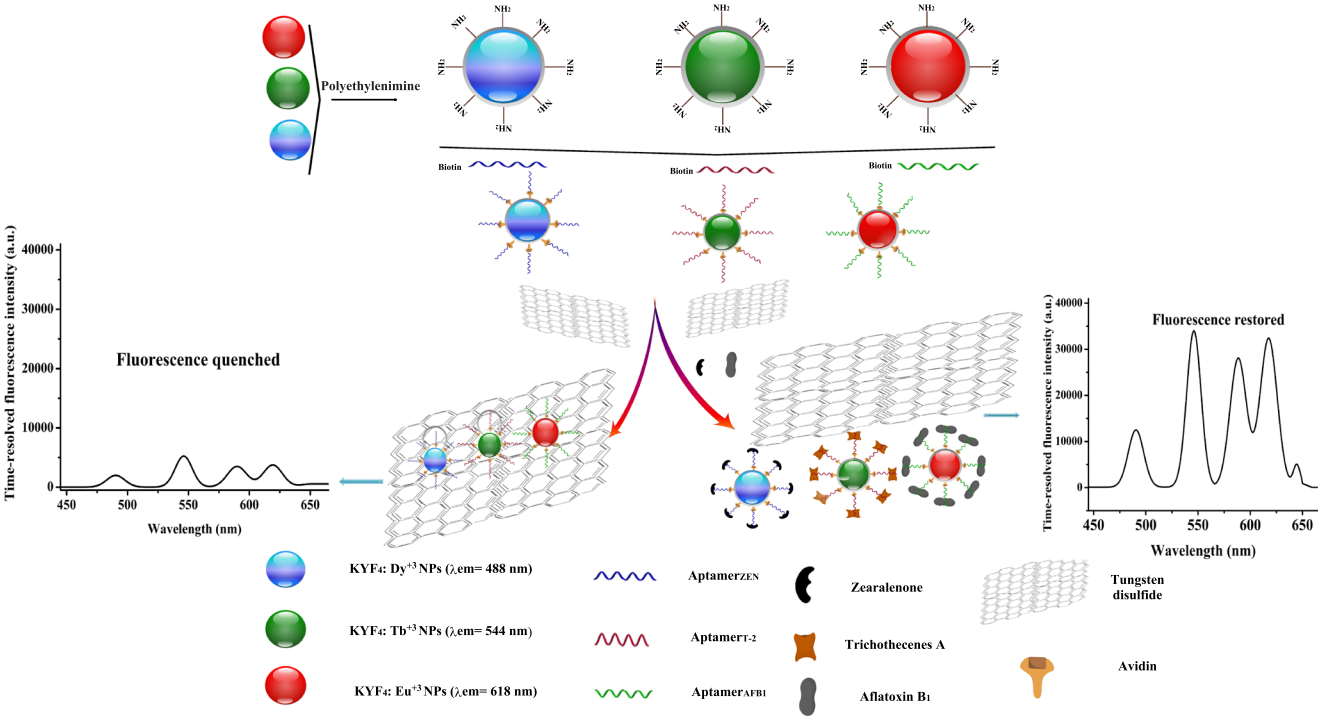

Fig. 1 Schematic demonstration of the time-resolved fluorescence based aptasensor for simultaneous detection of the mycotoxons zearalenone, trichothecenes A and aflatoxin B_1 using multicolor time-resolved fluorescence nanoparticles (KYF_4 NPs) as signal probe and tungsten disulfide as quencher

reagent Co., Ltd. (China) (http://www.sinoreagent.com). The tungsten disulfide (WS_2) nanosheet was bought from Nanjing XF Nano Material Tech Co., Ltd. (Nanjing, China). Avidin was purchased from Sangon Biotech Company (China) (http://www.sangon.com). The ZEN, T-2 and AFB_1 aptamers [23–25] were manufactured by Sangon Biotech Company (China) (http://www.sangon.com). The sequences of the ZEN, T-2 and AFB_1 aptamers were 5′-biotin-TCA TCT ATC TAT GGT ACA TTA CTA TCT GTA ATG TGA TAT G-3′, 5′-biotin-CAG CTC AGA AGC TTG ATC CTG TAT ATC AAG CAT CGC GTG TTT ACA CAT GCG AGA GGT GAA GAC TCG AAG TCG TGC ATC TG-3′, and 5′-biotin AGC AGC ACA GAG GTC AGA TGG TGC TAT CAT GCG CTC AAT GGG AGA CTT TAG CTG CCC CCA CCT ATG CGT GCT ACC GTG AA-3′, respectively.

Instrumentation

Powder XRD pattern was measured by a D8 Avance (Bruker AXS Ltd., Germany) with Cu-Kα radiation (λ = 0.1540 nm). TEM images of NPs were obtained by a JEOL model 2100 HR instrument (TEM, JEOL, Ltd., Japan) working at 200 kV accelerating voltage. The time-resolved fluorescence spectra (TRF) were measured by using a Synergy H1 multi-mode microplate reader (BioTek Instruments, Inc., Highland Park, USD) in time-resolved mode spectra scan with an excitation wavelength of 273 nm. UV-Vis absorption spectra were measurement by UV-1800 spectrophotometer (Shimadzu Co., Japan). The surface examination of WS_2 nanosheet was done by using a Dimension Icon Atomic Force Microscope System (AFM, Bruker Co., Germany).

Preparation of amine functionalized Ln^{3+} doped KYF_4 NPs

Ln^{3+} (Ln^{3+} = Dy^{3+}, Tb^{3+} and Eu^{3+}) doped KYF_4 NPs were prepared by one-step solothermal procedure [26] with some changes. The detail method is described in supporting information.

Preparation of aptamer modified KYF_4: Ln^{3+} multicolor bioprobe

First of all, avidin-modified KYF_4: Ln^{3+} NPs were obtained via earlier published classical glutaraldehyde procedure [14]. The avidin-functionalized KYF_4: Ln^{3+} NPs and 5′-Biotin-labeled aptamers were bounded through high affinity avidin-biotin system. The detail method is described in supporting information.

Procedure for simultaneous detection of mycotoxins

In the following experiment, ZEN aptamer modified KYF_4: Dy^{3+}, T-2 aptamer modified KYF_4: Tb^{3+} and AFB_1 aptamer

modified KYF_4: Eu^{3+} TR-FNPs (final concentration 1 mg mL^{-1}) were mixed with PBS (10 mmol mL^{-1} Na_2HPO_4, 137 mmol mL^{-1} NaCl, 2.7 mmol mL^{-1} KCl and 2 mmol mL^{-1} KH_2PO_4) followed by the addition of 0.3 mg mL^{-1} of WS_2 nanosheet solution at room temperature for 20 min. Then, various concentrations of targets solutions were added into above mixture to give the final volume of 200 μL to each well. The whole mixture was incubated for 40 min at 37 °C and then TRF emission spectra were measured using microplate reader. The conditions were set as follows; Synergy H1 multi-mode micro-plate reader in time-resolved mode at emission wavelengths of 488, 544 and 618 nm corresponded with Dy^{3+}, Tb^{3+} and Eu^{3+}, respectively, and an excitation wavelength of 273 nm, while the delay and gate times were set to be 100 μs and 1000 μs, respectively. All the intensity measurements were measured in triplicate.

Sample preparation

5 g of ground maize samples and 5 g of NaCl were put into a flask of 100 mL and then extracting solution (methanol + water; 7:3 (v:v)) was added into the flask upto the mark. The mixture was homogenized, stirred and extracted for 2 min. Next, the mixture was filtered and 10 mL of the filtrate was added into another flask (50 mL), followed by addition of water to the mark and mixed the whole mixture properly. The final mixture was filtered again using filter paper (glass fiber) to get very clear solution. The samples were used for standard addition and recovery experiment. The standard solutions of ZEN, T-2 and AFB_1 were added to the sample before adding the extracting solution.

Results and discussion

Detection scheme

Figure 1 illustrate the principle of this "turn on" fluorometric strategy. A sensitive aptasensor is presented for the simultaneous determination of ZEN, T-2 and AFB_1 based on the fluorescence quenching-restoration principle. The ZEN aptamer modified KYF_4: Dy^{3+}, T-2 aptamer modified KYF_4: Tb^{3+} and AFB_1 aptamer modified KYF_4: Eu^{3+} TRFNPs exhibited high fluorescence at 273 nm excitation wavelength. In the absence of targets, WS_2 is easily adsorbed by the mixing bioprobe via van der Waals forces between nucleobases and the WS_2 basal plane [22]. This brings the bioprobe and WS_2 into close proximity and results in quenched fluorescence. In the presence of targets, fluorescence of bioprobe restored because the targets react with DNA probe and modify their molecular conformation that weakened the interaction between the DNA and WS_2. Moreover, the weak affinity of WS_2 towards dsDNA leading the bioprobe to switch away from the surface of WS_2 resulted in strong fluorescence signal. Thus, a highly sensitive and specific recognition of ZEN, T-2 and AFB_1 were attained by measuring the fluorescence signals of the reaction system.

Characterization of Ln^{3+} doped KYF_4 NPs and WS_2

Ln^{3+} (Ln^{3+} = Dy^{3+}, Tb^{3+}, Eu^{3+}) doped KYF_4 NPs were prepared by one-step solothermal method with PEI as capping material. PEI was used to control the growth of the NPs and render them water soluble and surface functionalized for further linkage of biomolecule by bio-conjugate chemistry. TEM images (Fig. 2a) demonstrate monodispersity and uniformity of the NPs with an average diameter of about 25 nm. The XRD patterns (Fig. S1a) of NPs exhibit peaks position and intensities that can be well indexed to the pure cubic KYF_4 crystal [27] and no impurities or traces of other phases were identified, indicating high crystallinity of the NPs. Furthermore, the fluorescence emission spectra of separate (Fig. S1b, c & d) and combined (Fig. 2c) Ln^{3+} doped KYF_4 NPs were measured at 273 nm excitation wavelength. The Ln^{3+} (Ln^{3+} = Dy^{3+}, Tb^{3+}, Eu^{3+}) doped KYF_4 NPs display different emissions at 488 nm ($^4F_{9/2}$ to $^6H_{15/2}$) for Dy^{3+}, 544 nm ($^5D_4$ to $^7F_5$) for Tb^{3+} and 618 nm ($^5D_0$ to $^7F_2$) for Eu^{3+}.

The WS_2 nanosheets were characterized by TEM (Fig. 2b) and AFM (Fig. S2). The TEM and AFM images demonstrate the triangular shape and thickness of about 1.3 nm of WS_2, indicating the few-layer structure of nanosheet. Besides, there is a good overlap (Fig. 2d) between the broad absorption spectra of WS_2 nanosheet and emission spectra of multicolor TRF-NPs which present the good conditions for fluorescence quenching of TRF-NPs by WS_2 nanosheet.

Characterization of NPs conjugated to avidin and aptamers

The TRF-NPs were conjugated with avidin and aptamers, respectively. The UV-vis spectrophotometer was used to describe the avidin conjugated NPs. Fig. S3 shows the decrease in peak intensities at 280 nm after functionalized with avidin, indicating a successful attachment of avidin to NPs. Fig. S4 exhibits the weak peak intensities at 260 nm after functionalized with aptamers, representing a successful attachment of aptamers to NPs by avidin-biotin system.

Optimization of the aptasensor

The WS_2 nanosheet concentration has a significant effect on the fluorescence quenching. Therefore, the effect of WS_2 nanosheet concentration on time-resolved fluorescence intensity (TR-FI) was studied. As shown in the Fig. S5, different concentrations of WS_2 nanosheet ranging from 0.0 to

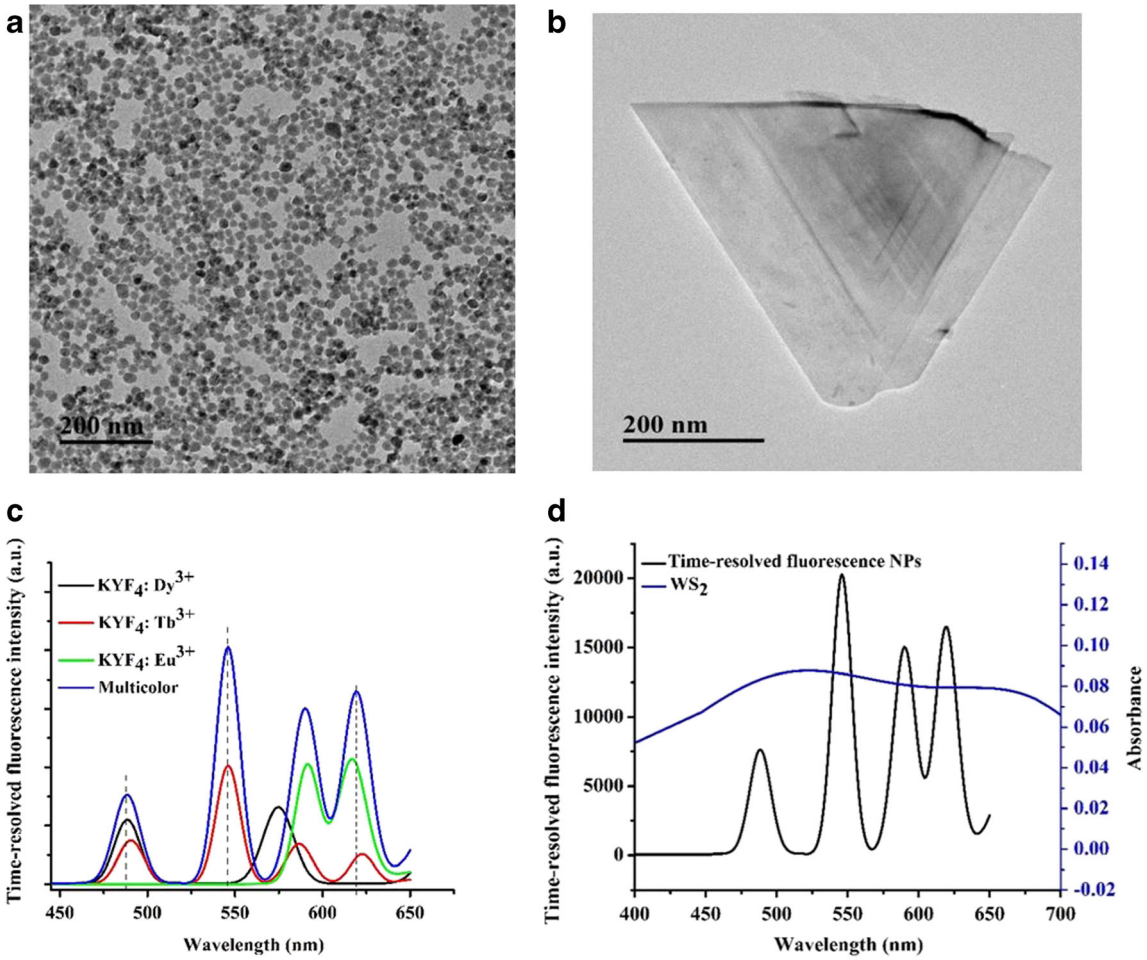

Fig. 2 TEM image of Ln^{3+} doped KYF_4 NPs (**a**), TEM image of WS_2 nanosheet (**b**), fluorescence emission spectra of mixture multi-color time-resolved fluorescence nanoparticles (**c**) and the overlap of absorption spectra of WS_2 and emission spectra of time-resolved fluorescence nanoparticles

0.5 mg mL^{-1} were used. The time-resolved fluorescence intensity (TR-FI) decreased gradually with the increase in the concentration of WS_2 from 0.01 to 0.2 mg mL^{-1} and then became stable from 0.3 to 0.5 mg mL^{-1} which shows the FI of aptasensor was quenched by the WS_2. Therefore, 0.3 mg mL^{-1} was used as optimized WS_2 concentration for following experiments.

In order to verify the quenching efficiency of WS_2 nanosheet, the WS_2 was incubated with three different fluorescent probes and the incubation time was investigated. As shown in the Fig. S6, the fluorescence intensity for KYF_4: Dy^{3+} bioprobe incubated with WS_2 was quenched after 15 min while the fluorescence intensities for KYF_4: Tb^{3+} and KYF_4: Eu^{3+} bioprobes incubated with WS_2 were quenched after 20 min. Considering the three mycotoxins detected in the same system, 20 min was selected as optimized incubation time for fluorescence quenching by WS_2 for the subsequent experiments.

Furthermore, the interference tests for ZEN, T-2 and AFB_1 were performed separately using multicolor aptasensor. Firstly, the proper ratio of the three color bioprobes (Dy^{3+}, Tb^{3+}, Eu^{3+} = 3: 1: 2) was adjusted to make multicolor bioprobe. The multicolor bioprobe was incubated with WS_2 for 20 min and then 1 ng mL^{-1} of each mycotoxins was added separately. The whole mixture was incubated for 40 min at 37 °C. Then TRF emission spectra were measured. As shown in the Fig. 3a–c, in the absence of ZEN, T-2 and AFB_1 the original FI of mixing bioprobes was significantly quenched by WS_2 (red curve). When ZEN was added separately to the sensing probe, the FI of the respective probe (at 488 nm) was restored (Fig. 3a), while FI of other probes were almost quenched. Similarly, when T-2 and AFB_1 were added separately to the sensing probe, the FI of their respective probes at 544 nm (Fig. 3b) and 618 nm (Fig. 3c) respectively, were restored while FI of other probes were still quenched. The result indicated that there is a clear difference between the emission spectra of bioprobes incubated with respective target and bioprobes incubated with WS_2. It has been confirmed that the bioprobes with NPs of multi-color fluorescence emission can distinguish among the three mycotoxins and can detected three mycotoxins simultaneously without interfering each other. Consequently, the aptasensor has potential to detect ZEN, T-2 and AFB_1 individually and simultaneously.

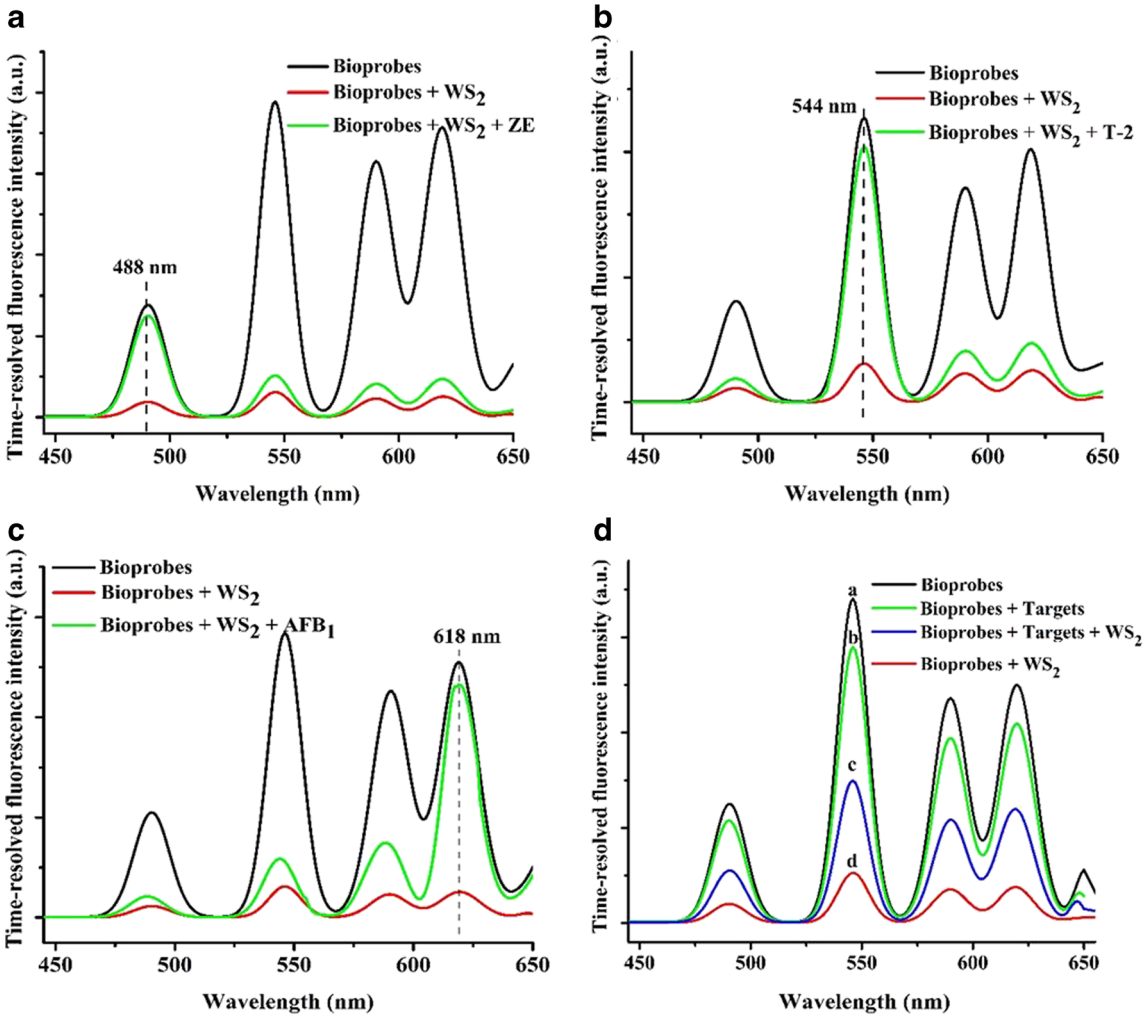

Fig. 3 The measurement of fluorescence emission spectra of multi-color bioprobe for ZEN (**a**) T-2 (**b**) and AFB_1 (**c**), separately and emission spectra of mixed multi-color bioprobes (**d**) at different conditions; bioprobes (curve a), bioprobes incubated with targets (curve b), bioprobes incubated with WS_2 and also with targets (curve c) and bioprobes only incubated with WS_2 (curve d), respectively

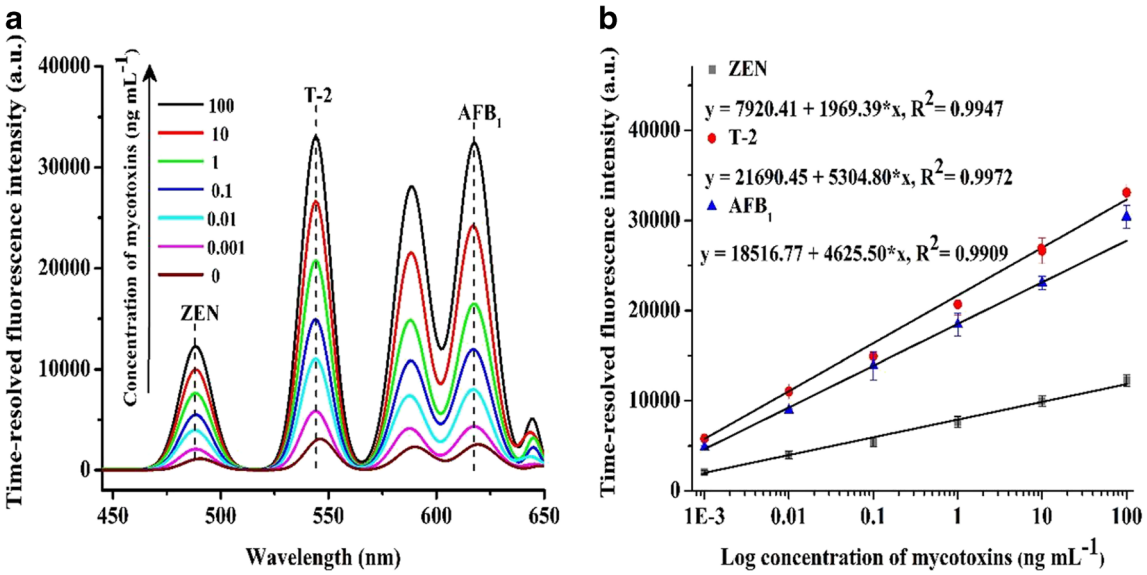

Fig. 4 Fluorescence emission spectra (**a**) and standard curve (**b**) for simultaneous detection of three mycotoxins

Moreover, the feasibility of the aptasensor was proved by examining the fluorescence spectra of detection solutions at different conditions as shown in Fig. 3d. The strong fluorescence of bioprobes (curve a) was quenched by WS_2 nanosheet (curve d). However, the fluorescence signals were restored after the addition of targets due to the removal of bond between DNA and WS_2 (curve c). Besides, in the absence of WS_2, the presence of target slightly affects the fluorescence (curve b) indicating that the target itself does not have significant effect on the fluorescence of bioprobe. The above results verified the feasibility of the aptasensor.

Analytical performance

In our control experiment, three emissions at 488, 544 and 618 nm for Dy^{3+}, Tb^{3+} and Eu^{3+} were selected for simultaneous quantification of ZEN, T-2 and AFB_1, respectively. Based on the optimized conditions, various concentrations (0.001–100 ng mL^{-1}) of ZEN, T-2 and AFB_1 were detected. As shown in the Fig. 4a, increase in the TRF intensities was proportional to the increase in the concentrations of mycotoxins because more target bind with TRFNPs-Apt, more TRFNPs-Apt switched away from the surface of WS_2 nanosheet resulted in enhanced FI. Figure 4b shows a linear relationship between the TRF intensity (F.I) and log concentration of targets. A strong linear correlation ($R^2 = 0.9947$, y = 7920.41 + 1969.39*x) between the F.I at 488 nm and log concentration of ZEN was observed. There is also a good linear relationship between the F.I at 544 nm ($R^2 = 0.9972$, y = 21,690.45 + 5304.80*x) and 618 nm ($R^2 = 0.9909$, y = 18,516.77 + 4625.50*x) and log concentration of T-2 and AFB_1, respectively were noted. The results suggested that aptasensor can be applied for simultaneous detection of ZEN, T-2 and AFB_1.

The sensitivity of the aptasensor was also observed. Statistical results exhibited that the limit of detection (LOD) of ZEN, T-2 and AFB_1 were 0.51 pg mL^{-1}, 0.33 pg mL^{-1} and 0.40 pg mL^{-1}, respectively, which is lower than others reported methods. A comparison table (Table 1) is given between our aptasensor and earlier methods for ZEN, T-2 and AFB_1 detection. It demonstrates that our method for simultaneous recognition of ZEN, T-2 and AFB_1 has wider working range and lower LOD than others methods. The above findings proved that our method is highly efficient and sensitive.

Selectivity of assay

In order to test the selectivity of the aptasensor, the five mycotoxins including OTA, FB_1, AFB_2, DON and Patulin were added to the sample solution as interferences. In our research, specificity of aptasensor is highly depends on aptamers. The change in the fluorescence intensity (ΔF.I) was measured by following the same method as used for simultaneous detection

Table 1 Comparison between our method and different analytical methods for individual and simultaneous detection of ZEN, T-2 and AFB_1

Analyte	Matrix	Technique	Response range	LOD	Reference
ZEN	Corn & beer	UCNPs based aptasensor	0.05–100 μg L^{-1}	0.007 μg L^{-1}	[28]
	Maize and wheat	Time-resolved NPs	0.001–10 ng mL^{-1}	0.21 pg mL^{-1}	[29]
T-2	Miaze & wheat	Silver nanoclusters based FRET aptasensor	0.005–500 ng mL^{-1}	0.93 pg mL^{-1}	[30]
	Shrimp tissues	IMB-ELISA	5–75 ng mL^{-1}	2.53 ng mL^{-1}	[8]
AFB_1	Cottonseed meal & corn	Eu-Nano-TRFIA	0.48–30.0 μg kg^{-1}	0.16 μg kg^{-1}	[31]
	Peanuts, corn, soy sauce, vegetable oil, & mouse feed	Chromatographic TR fluoroimmunoassay	0.2–60 μg kg^{-1}	0.06 to 0.12 μg kg^{-1}	[32]
	Soybean sauce	TRF-immunochromatographic strip test	0.3–10.0 μg kg^{-1}	0.1 μg kg^{-1}	[10]
	Red wine & beer	Surface plasmon resonance (SPR) based aptasensor	0.4 nM to 200 nM	0.4 nM	[33]
	Peanut oil	Aptamer based fluorescence assay	3.2 nM to 320 μM	1.0 nM	[34]
AFB_1 & ZEN	Maize	TRFICA	0.13–4.54 ng mL^{-1} for AFB & 0.20–2.77 ng mL^{-1} for ZEN	0.05 and 0.07 ng mL^{-1} for AFB_1 & ZEN respectively	[35]
T-2, AFB_1, OTA, & ZEN	Water & corn	Immunoassay	0.1–20 ng mL^{-1}	0.03 and 1.24 ng mL^{-1}	[2]
ZEN, T-2 & AFB_1	Maize	TR-aptasensor	0.001–100 ng mL^{-1}	0.51, 0.33 & 0.40 pg mL^{-1} for ZEN T-2 & AFB_1, respectively	Present work

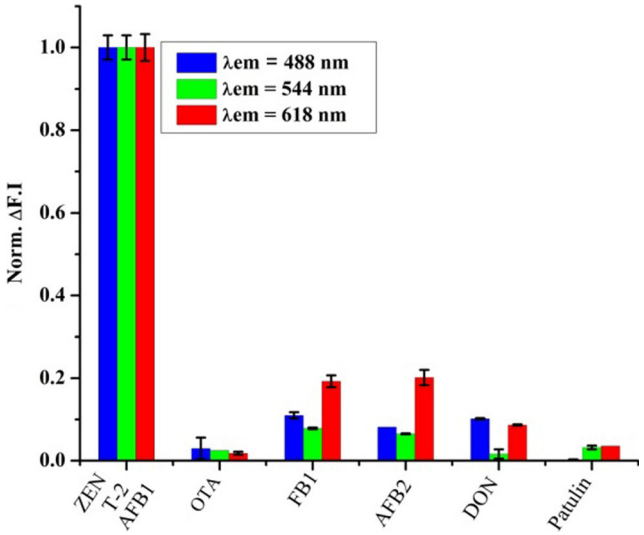

Fig. 5 Selectivity of aptasensor with various mycotoxins as interferents. All the measurements were done in three replicates

of ZEN, T-2 and AFB_1. Herein, $\Delta F.I = F–F_0$ where F and F_0 were the fluorescence intensities at 488, 544 and 618 nm in the presence and absence (Probe + WS_2) of targets. The fix concentration of 0.1 ng mL^{-1} for all the mycotoxins was interrogated. Figure 5 shows that no obvious change in the fluorescent response was detected when the interferences were in the sample. In contrast, very strong fluorescence intensities were detected when ZEN, T-2 or AFB_1 were in the sample. These results clearly indicated that the aptasensor has suitable selectivity for ZEN, T-2 and AFB_1 detection which was credited to the characteristic and high specificity of the aptamers toward ZEN, T-2 and AFB_1.

Real food sample analysis

To explore the effectiveness of the aptasensor, tests for ZEN, T-2 and AFB_1 were performed in maize sample to measure the recoveries by standard addition method. The samples were tested by ZEN, T-2 and AFB_1 ELISA test kits to confirm that maize samples were not contaminated with ZEN, T-2 and AFB_1. The samples were spiked with 0.05, 0.5, 5 and 50 ng mL^{-1} ZEN, T-2 and AFB_1. The spiked samples were examined by new method and ELISA method to detect ZEN, T-2 and AFB_1. The recovery results are summarized in Table S1. The recoveries obtained from our method for ZEN, T-2 and AFB_1 were in the range of 94.4–98.0%, 90.0–92.0% and 87.0–96.0%, respectively. The recoveries obtained from ELISA for ZEN, T-2 and AFB_1 were in the range of 98.0–102%, 92.2–100% and 96.0–112%, respectively. These results confirm the fluorescent assay as a suitable recognition method. Moreover, the results shown in Fig.S7 indicate that there is no significant difference between two methods and they are particularly correlated. The results indicate that the aptasensor can be applied to the determination of ZEN, T-2 and AFB_1 in agricultural products.

Conclusion

We report that the unique interaction between WS_2 and DNA can be used to construct time-resolved fluorescence nanoparticles based aptasensor for simultaneous recognition of ZEN, T-2 and AFB_1. The present method has several significant features. First, it uses the strong fluorescence emission and long luminescence lifetimes of time-resolved fluorescence nanoparticles. Second, it uses extraordinarily high fluorescence quenching efficiency of WS_2 which is very important for the sensitivity of quenching and recovery based biosensor. This aptasensor showed high selectivity, sensitivity and stability owing to the unique WS_2 to DNA interaction and the definite aptamer to target recognition. Moreover, the detection limit of present aptasensor was much lower than most other reported assays and also homogeneous assay design made the method convenient without washing and separation steps. However, the method requires several operational steps and important nanotechnology skills in order to be reproduced by others. Conversely, it would be easy to simplify this strategy to detect the multiple targets using different aptamers.

Acknowledgements This work was partly funded by the National Natural Science Foundation of China (31871881), Zhangjiagang Science and Technology Support plan (Social development) (ZKS 1803), Jiangsu Agriculture Science and Technology Innovation Fund (JASTIF) (CX (18)2025), S&T Support Program of Jiangsu Province (BE2017623), the National First-class Discipline Program of Food Science and Technology (JUFSTR20180303), JUSRP51714B and the Distinguished Professor Program of Jiangsu Province.

Compliance with ethical standards The author(s) declare that they have no competing interests.

References

1. Grenier B, Oswald I (2011) Mycotoxin co-contamination of food and feed: meta-analysis of publications describing toxicological interactions. World Mycotoxin J 4(3):285–313. https://doi.org/10.3920/WMJ2011.1281
2. Chen Y, Meng X, Zhu Y, Shen M, Lu Y, Cheng J, Xu Y (2018) Rapid detection of four mycotoxins in corn using a microfluidics and microarray-based immunoassay system. Talanta 186:299–305. https://doi.org/10.1016/j.talanta.2018.04.064
3. Sun Y, Hu X, Zhang Y, Yang J, Wang F, Wang Y, Deng R, Zhang G (2014) Development of an immunochromatographic strip test for the rapid detection of zearalenone in corn. J Agric Food Chem 62(46):11116–11121. https://doi.org/10.1021/jf503092j
4. Gao X, Cao W, Chen M, Xiong H, Zhang X, Wang S (2014) A high sensitivity electrochemical sensor based on Fe^{3+}-ion molecularly imprinted film for the detection of T-2 toxin. Electroanal 26(12):2739–2746. https://doi.org/10.1002/elan.201400237

5. Ma Y, Mao Y, Huang D, He Z, Yan J, Tian T, Shi Y, Song Y, Li X, Zhu Z (2016) Portable visual quantitative detection of aflatoxin B 1 using a target-responsive hydrogel and a distance-readout microfluidic chip. Lab Chip 16(16):3097–3104 https://pubs.rsc.org/en/content/articlehtml/2016/lc/c6lc00474a
6. Solfrizzo M, Gambacorta L, Lattanzio VM, Powers S, Visconti A (2011) Simultaneous LC–MS/MS determination of aflatoxin M 1, ochratoxin a, deoxynivalenol, de-epoxydeoxynivalenol, α and β-zearalenols and fumonisin B 1 in urine as a multi-biomarker method to assess exposure to mycotoxins. Anal Bioanal Chem 401(9):2831. https://link.springer.com/article/10.1007/s00216-011-5354-z–2841
7. Tokuşoğlu Ö, Ünal MK, Yemiş F (2005) Determination of the phytoalexin resveratrol (3, 5, 4 '-trihydroxystilbene) in peanuts and pistachios by high-performance liquid chromatographic diode array (HPLC-DAD) and gas chromatography− mass spectrometry (GC-MS). J Agric Food Chem 53(12):5003–5009. https://doi.org/10.1021/jf050496+
8. Deng Q, Qiu M, Wang Y, Lv P, Wu C, Sun L, Ye R, Xu D, Liu Y, Gooneratne R (2017) A sensitive and validated immunomagnetic-bead based enzyme-linked immunosorbent assay for analyzing total T-2 (free and modified) toxins in shrimp tissues. Ecotoxicol Environ Saf 142:441–447 https://www.sciencedirect.com/science/article/pii/S0147651317302476
9. Zhang Z, Wang D, Li J, Zhang Q, Li P (2015) Monoclonal antibody–europium conjugate-based lateral flow time-resolved fluoroimmunoassay for quantitative determination of T-2 toxin in cereals and feed. Anal Methods 7(6):2822–2829 https://pubs.rsc.org/en/content/articlehtml/2015/ay/c5ay00100e
10. Wang D, Zhang Z, Li P, Zhang Q, Zhang W (2016) Time-resolved fluorescent immunochromatography of aflatoxin b1 in soybean sauce: a rapid and sensitive quantitative analysis. Sens 16(7):1094 https://www.mdpi.com/1424-8220/16/7/1094
11. Liu Y, Tu D, Zhu H, Chen X (2013) Lanthanide-doped luminescent nanoprobes: controlled synthesis, optical spectroscopy, and bioapplications. Chem Soc Rev 42(16):6924–6958 https://pubs.rsc.org/en/content/articlehtml/2013/cs/c3cs60060b
12. Li F, Zhang H, Wang Z, Newbigging AM, Reid MS, Li X-F, Le XC (2014) Aptamers facilitating amplified detection of biomolecules. Anal Chem 87(1):274–292. https://doi.org/10.1021/ac5037236
13. Zhou W, Huang P-JJ, Ding J, Liu J (2014) Aptamer-based biosensors for biomedical diagnostics. Anal 139(11):2627–2640 https://pubs.rsc.org/en/content/articlehtml/2014/an/c4an00132j
14. Huang Y, Zhang H, Chen X, Wang X, Duan N, Wu S, Xu B, Wang Z (2015) A multicolor time-resolved fluorescence aptasensor for the simultaneous detection of multiplex Staphylococcus aureus enterotoxins in the milk. Biosens Bioelectron 74:170–176. https://doi.org/10.1016/j.bios.2015.06.046
15. Huang Y, Chen X, Wu S, Duan N, Yu Y, Wang Z (2015) Homogeneous time-resolved fluorescence assay for the detection of ricin using an aptamer immobilized on europium-doped $KGdF_4$ nanoparticles and graphene oxide as a quencher. Microchim Acta 182(5–6):1035–1043. https://doi.org/10.1007/s00604-014-1422-3
16. Wang X, Niazi S, Yukun H, Sun W, Wu S, Duan N, Hun X, Wang Z (2017) Homogeneous time-resolved FRET assay for the detection of Salmonella typhimurium using aptamer-modified $NaYF_4$: Ce/Tb nanoparticles and a fluorescent DNA label. Microchim Acta 184(10):4021–4027. https://doi.org/10.1007/s00604-017-2399-5
17. Voiry D, Yamaguchi H, Li J, Silva R, Alves DC, Fujita T, Chen M, Asefa T, Shenoy VB, Eda G (2013) Enhanced catalytic activity in strained chemically exfoliated WS_2 nanosheets for hydrogen evolution. Nat Mater 12(9):850. https://www.nature.com/articles/nmat3700–855
18. Qin Y, Ma Y, Jin X, Zhang L, Ye G, Zhao S (2015) A sensitive fluorescence turn-on assay of bleomycin and nuclease using WS2 nanosheet as an effective sensing platform. Anal Chim Acta 866:84–89. https://doi.org/10.1016/j.aca.2015.01.049
19. Lin T, Zhong L, Song Z, Guo L, Wu H, Guo Q, Chen Y, Fu F, Chen G (2014) Visual detection of blood glucose based on peroxidase-like activity of WS_2 nanosheets. Biosens Bioelectron 62:302–307. https://doi.org/10.1016/j.bios.2014.07.001
20. Ge J, Du Y-H, Chen J-J, Zhang L, Bai D-M, Ji D-Y, Hu Y-L, Li Z-H (2017) Highly sensitive fluorescence detection of mercury (II) ions based on WS2 nanosheets and T7 exonuclease assisted cyclic enzymatic amplification. Sensors Actuators B Chem 249:189–194. https://doi.org/10.1016/j.snb.2017.04.094
21. Zuo X, Zhang H, Zhu Q, Wang W, Feng J, Chen X (2016) A dual-color fluorescent biosensing platform based on WS2 nanosheet for detection of Hg^{2+} and Ag^{+}. Biosens Bioelectron 85:464–470. https://doi.org/10.1016/j.bios.2016.05.044
22. Xi Q, Zhou D-M, Kan Y-Y, Ge J, Wu Z-K, Yu R-Q, Jiang J-H (2014) Highly sensitive and selective strategy for microRNA detection based on WS2 nanosheet mediated fluorescence quenching and duplex-specific nuclease signal amplification. Anal Chem 86(3):1361–1365. https://doi.org/10.1021/ac403944c
23. Chen X, Huang Y, Duan N, Wu S, Ma X, Xia Y, Zhu C, Jiang Y, Wang Z (2013) Selection and identification of ssDNA aptamers recognizing zearalenone. Anal Bioanal Chem 405(20):6573–6581. https://doi.org/10.1007/s00216-013-7085-9
24. Chen X, Huang Y, Duan N, Wu S, Xia Y, Ma X, Zhu C, Jiang Y, Wang Z (2014) Screening and identification of DNA aptamers against T-2 toxin assisted by graphene oxide. J Agric Food Chem 62(42):10368–10374. https://doi.org/10.1021/jf5032058
25. Ma X, Wang W, Chen X, Xia Y, Wu S, Duan N, Wang Z (2014) Selection, identification, and application of aflatoxin B1 aptamer. Eur Food Res Technol 238(6):919–925. https://doi.org/10.1007/s00217-014-2176-1
26. Ju Q, Tu D, Liu Y, Li R, Zhu H, Chen J, Chen Z, Huang M, Chen X (2011) Amine-functionalized lanthanide-doped KGdF4 nanocrystals as potential optical/magnetic multimodal bioprobes. J Am Chem Soc 134(2):1323–1330. https://doi.org/10.1021/ja2102604
27. Schäfer H, Ptacek P, Zerzouf O, Haase M (2008) Synthesis and optical properties of KYF4/Yb, Er nanocrystals, and their surface modification with undoped KYF_4. Adv Funct Mater 18(19):2913–2918. https://doi.org/10.1002/adfm.200800368
28. Wu Z, Xu E, Chughtai MF, Jin Z, Irudayaraj J (2017) Highly sensitive fluorescence sensing of zearalenone using a novel aptasensor based on upconverting nanoparticles. Food Chem 230:673–680. https://doi.org/10.1016/j.foodchem.2017.03.100
29. Niazi S, Wang X, Pasha I, Khan IM, Zhao S, Shoaib M, Wu S, Wang Z (2018) A novel bioassay based on aptamer-functionalized magnetic nanoparticle for the detection of zearalenone using time resolved-fluorescence $NaYF_4$: Ce/Tb nanoparticles as signal probe. Talanta 186:97–103. https://doi.org/10.1016/j.talanta.2018.04.013
30. Khan IM, Zhao S, Niazi S, Mohsin A, Shoaib M, Duan N, Wu S, Wang Z (2018) Silver nanoclusters based FRET aptasensor for sensitive and selective fluorescent detection of T-2 toxin. Sensors Actuators B Chem 277:328–335. https://doi.org/10.1016/j.snb.2018.09.021
31. Wang D, Zhang Z, Li P, Zhang Q, Ding X, Zhang W (2015) Europium nanospheres-based time-resolved fluorescence for rapid and ultrasensitive determination of total aflatoxin in feed. J Agric Food Chem 63(47):10313–10318. https://doi.org/10.1021/acs.jafc.5b03746
32. Zhang Z, Tang X, Wang D, Zhang Q, Li P, Ding X (2015) Rapid on-site sensing aflatoxin B1 in food and feed via a chromatographic

time-resolved fluoroimmunoassay. PLoS One 10(4):e0123266. https://doi.org/10.1371/journal.pone.0123266

33. Sun L, Wu L, Zhao Q (2017) Aptamer based surface plasmon resonance sensor for aflatoxin B1. Microchim Acta 184(8):2605–2610. https://doi.org/10.1007/s00604-017-2265-5
34. Lu Z, Chen X, Wang Y, Zheng X, Li CM (2015) Aptamer based fluorescence recovery assay for aflatoxin B1 using a quencher system composed of quantum dots and graphene oxide. Microchim Acta 182(3–4):571–578. https://doi.org/10.1007/s00604-014-1360-0
35. Tang X, Li P, Zhang Q, Zhang Z, Zhang W, Jiang J (2017) Time-resolved fluorescence immunochromatographic assay developed using two idiotypic nanobodies for rapid, quantitative, and simultaneous detection of aflatoxin and zearalenone in maize and its products. Anal Chem 89(21):11520–11528. https://doi.org/10.1021/acs.analchem.7b02794